Available online at www.sciencedirect.com
SCIENCE DIRECT
Cement and Concrete Research 36 (2006) 576 – 583
Cement and Concrete Research

Fracture parameters for high-performance concrete

Ricardo A. Einsfeld [a], Marta S.L. Velasco [b,*]

[a] Polytechnic Institute (IPRJ), State University of Rio de Janeiro (UERJ), P.O. Box 97282, 28601-970, Nova Friburgo, RJ, Brazil
[b] Department of Civil Engineering, Pontifical Catholic University of Rio de Janeiro (PUC-Rio), 22451-900, Rio de Janeiro, RJ, Brazil

Received 16 September 2005; accepted 17 September 2005

Abstract

This paper reports and discusses the results of an experimental investigation on fracture properties of high-performance concrete, involving the tests of 115 three-point bend specimens with different compression strengths. The parameters were obtained by the work-of-fracture method and by the size effect method. For most series of tests the fracture energy was measured by the two methods, allowing a correlation between the values obtained by the two processes. A comparison with some results found in literature was performed. It was found that: (a) the ratio between the fracture energy measured by the work-of-fracture method (G_F) and by the size effect method (G_f) matched the value estimated by other researchers ($G_F/G_f \approx 2.5$); (b) generally, G_F increases as the concrete compressive strength increases; and (c) the values obtained for G_f showed a slight trend to decrease with increasing compressive strength. The results obtained from the standard compressive strength tests indicate that the concrete strength was limited by the type and size of the coarse aggregate. The objective of this study is to provide some experimental data that can be useful in engineering practice for calibrating numerical constitutive models.

Keywords: High-performance concrete; Fracture energy; Brittleness number; Size effect

1. Introduction

The increasing use of high-performance concrete (HPC) in conventional structures has been demanding more attention from researchers and engineers in order to establish the correct application of this material in civil construction. For the past two decades the fracture properties of concretes with inclusion of mineral components in its matrix structure, as HPC and high-strength concrete (HSC), has been investigated world-wide. Differences in relation to conventional concrete have been emphasized with regard to the design and safety assessment of HPC/HSC structures. The fracture behavior of structures designed with HPC is characterized by its high brittleness caused by its internal damage pattern, when most cracks extend through the coarse aggregates.

Investigations in this area of research have been conducted by the authors at the Department of Civil Engineering at PUC-Rio in order to study the fracture properties of HPC. A total of 115 beam specimens have been submitted to three-point bend tests at the Technological Institute at PUC (ITUC) using closed-loop servo-controlled testing machines. The fracture parameters were obtained by the work-of-fracture method, according to RILEM Draft Recommendation 50-FMC [1] and by the size effect method, according to RILEM Draft Recommendation TC89-FMT [2]. For most series of tests the fracture energy was measured by the two methods, allowing a correlation between the values obtained by the two processes. The results obtained in the tests were analyzed and compared with results found in literature.

The objective of this study is to characterize the brittle behavior of the HPC in order to establish adequate safety criteria for the material utilization. The parameters obtained in the experiments can provide a database for calibrating of numerical models and the development of design criteria for HPC structures.

2. Determination of fracture parameters

In order to determine the fracture energy, one can apply the recommendation of the Technical Committee RILEM 50-FMC [1] to perform three-point bend tests in notched beams. The fracture energy is defined as the amount of energy necessary to

* Corresponding author. Tel.: +55 21 3114 1188; fax: +55 21 3114 1194.
E-mail address: marta@civ.puc-rio.br (M.S.L. Velasco).

0008-8846/$ - see front matter © 2005 Elsevier Ltd. All rights reserved.
doi:10.1016/j.cemconres.2005.09.004

create a crack of unit surface area projected in a plane parallel to the crack direction. As the beam is split in two halves, the fracture energy can be determined dividing the total dissipated energy by the total surface area of the crack:

$$G_F = \frac{W}{b(d - a_0)} \quad (1)$$

where W is the total energy dissipated in the test, b is the thickness, d is the height and a_0 is the notch depth of the beam, respectively.

According to Bazant and Pfeiffer [3], the method proposed by RILEM, also known as work-of-fracture method or Hillerborg's method [4], delivers materials fracture characteristics which are ambiguous and, especially, size-dependent. As a consequence, different values for the fracture energy are obtained for specimens of different sizes. In an alternative method proposed by Bazant and Pfeiffer, the fracture energy is determined from the size effect law. In this case, by definition, the value of the fracture energy is independent of the size of the specimens. If geometrically similar beams are used and the load at rupture extrapolated to a beam of infinite dimensions, the fracture energy must have one single value, regardless the type, size or shape of the specimen. This procedure is known as the size effect method (SEM).

Through this asymptotic approach, the problem is now reduced to find and apply the correct law for the size effect. Bazant and Pfeiffer suggested the following relationship:

$$\sigma_N = B\left(1 + \beta^k\right)^{\frac{-1}{2k}} \quad (2)$$

where σ_N is the nominal stress at failure, B is a coefficient obtained through the linear regression plot of the test results, β is the brittleness number and k is a parameter which can be optimized for a most accurate representation of the size effect. Nevertheless, according to Bazant and Pfeiffer, no case was found in practice in which this optimization had been necessary, and usually the value of $k=1$ is applied.

The nominal stress is obtained from the experimental tests as:

$$\sigma_N = C_n \frac{P_u}{bd} \quad (3)$$

where P_u is the ultimate load and C_n is a coefficient introduced for convenience.

The brittleness number indicates whether the behavior of any structure is related to limit state analysis or to linear elastic fracture mechanic (LEFM) analysis. Bazant and Pfeiffer propose the following equation for the brittleness number:

$$\beta = \frac{d}{d_0} \quad (4)$$

where d is the characteristic dimension of the structure (the specimen height in this study) and d_0 is a coefficient determined experimentally.

The value of $\beta=1$ corresponds to the transition point between the strength approach and the LEFM approach. For values of $\beta \leq 0.1$, the plastic limit analysis should be used for structural design, and for values of $\beta \geq 10$, the LEFM should be used. For $0.1 < \beta < 10$, the nonlinear fracture mechanics should be used for structural design.

The coefficients B and d_0 in Eqs. (2) and (4), respectively, are determined by linear regression. For this purpose, Eq. (2), applicable to geometrically similar specimens of different sizes, can be algebraically rearranged to a linear regression plot $Y=AX+C$, in which:

$$Y = (1/\sigma_N)^2; \quad X = d; \quad d_0 = C/A; \quad B = 1/\sqrt{C} \quad (5)$$

Rupture of a structure of infinite size follows the LEFM theory, since the plastic region around the concrete fracture zone is relatively small. In this case, the fracture energy can be calculated as:

$$G_f = \frac{g_f(\alpha_0)}{AE} \quad (6)$$

where E is the Young's elastic modulus of the concrete, A is the angular coefficient of the linear regression plot, $g_f(\alpha_0)$ is the non-dimensional energy release rate calculated according to LEFM and found in many books as Anderson [5], and α_0 is the relative notch length (a_0/d).

3. Experimental study

Three-point bend tests for HPC notched beams were performed to determine the fracture parameters. The experimental study was chronologically divided into three different Stages (Stages 1 to 3), where different methodologies and test arrangements were applied. Table 1 shows the concrete mixes

Table 1
Concrete composition

	Mix designation (volume of mix per 1 m^3)				
	HP1	HP2	HP3	HP4	HP5
Target compressive strength at 28 days (MPa)	50	60	70	90	110
Max size of aggregate (mm)	9.5	9.5	9.5	9.5	9.5
Cement (kg)	399	456	420	457	540
Sand (kg)	872	820	860	814	724
Gravel (kg)	992	992	992	992	992
Water (kg)	151	152	147	153	151
Microsilica (kg)	44	50	47	50	60
Superplasticizer (ℓ)	8.2	9.0	11.5	12.4	14.8
Water–cementitious materials (w/cm) ratio	0.34	0.30	0.31	0.30	0.25

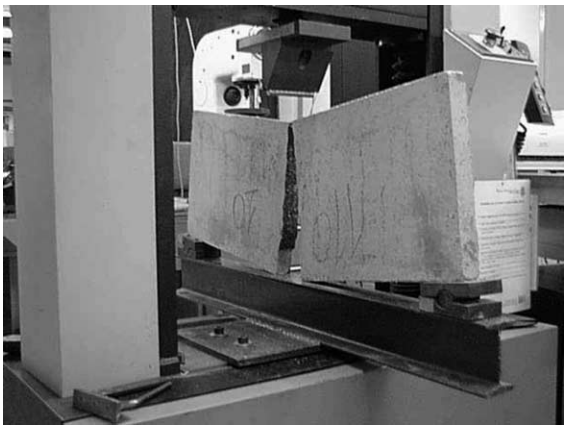

Fig. 1. Test set-up using a closed-loop servo-controlled Instron testing machine model 5500 R. Specimen with $d=304.8$ mm.

used in this study. All tests were performed at the Technological Institute at PUC (ITUC) using closed-loop servo-controlled testing machines equipped with load cells of 25 kN and 50 kN capacity. A photograph of the test set-up for Stage 2 is shown in Fig. 1.

3.1. Results of stage 1

In Stage 1 [6], two batches of concrete for molding two sets of beams with six specimens each were used. The dimensions of all beams were $100\times100\times840$ mm (height × depth × length), with a span of 800 mm. The details of the concrete mixes, labeled HP1 and HP2 for batches 1 and 2, respectively, are given in Table 1. The proportions, by weight, of cement/sand/gravel/water/microsilica were 1:2.18:2.49:0.38:0.11 and 1:1.80:2.17:0.33:0.11 for mixes HP1 and HP2, respectively. Brazilian cement CP-32 (equivalent to ASTM Type I) was used at this Stage. The fine aggregate was natural river sand passing through a 2.4-mm sieve. The coarse aggregate was crushed gneiss with maximum size (d_a) equal to 9.5 mm. A melamine sulphonate-type superplasticizer (Sikament 300) was used.

Along with the beam specimens, six 100×200 mm cylinders were cast for each concrete batch. The cylinders corresponding to mixes HP1 and HP2 were tested after 70 and 75 days, at the same day as the corresponding set of beams, and failed at an average maximum compressive stress of 48 MPa (±3.0%) and 49 MPa (±1.8%), respectively.

Before testing the beam specimens, a notch of half depth was saw-cut at the mid-section of the beam. The tests were controlled by the vertical displacement at the load cell. A closed-loop servo-controlled Instron testing machine model 5500 R equipped with two channels for data acquisition and a load cell of 25 kN capacity was used. The complete load–deflection curves were recorded for all the tests. Table 2 shows the values obtained for the fracture energy according to the work-of-fracture method for the two Series of tests (A1 and A2). The values marked with an asterisk were higher than expected and were not considered to measure the average G_F and the corresponding coefficient of variation. The tests were conducted as described in the RILEM 50-FMC [1] guidelines. The total energy dissipated in the test was given by $W=W_0+mgu_f$, where W_0 is the area under the load–deflection curve, mg is the weight of the specimen and u_f corresponds to the deflection when the beam fractures completely. Deflection u_f was taken equal to 10% of the measured peak load. In order to measure G_F, the load–deflection curves were corrected for eventual non-linearities due to specimen deformation at the load point and the supports, as recommended in the RILEM guidelines.

3.2. Results of stage 2

In Stage 2 [7], geometrically similar specimens with four different sizes were used in order to allow the fracture energy evaluation through the SEM besides the work-of-fracture method. The specimens had depths (d) of 38.1, 76.2, 152.4 and 304.8 mm, with the same thickness (b) of 38.1 mm, lengths equal to $2.67d$, and span equal to $2.5d$. A total of 60 specimens, divided in five Series of concrete batches (Series B1 to B5), were cast. Each Series contains three specimens for each of the four heights. The concrete mixes HP3, HP4 and HP5 were used in this Stage. The details of the concrete composition are given in Table 1. The proportions, by weight, of cement/sand/gravel/water/microsilica were 1:2.05:2.36:0.35:0.11, 1:1.78:2.17:0.33:0.11 and 1:1.34:1.84:0.28:0.11, for mixes HP3, HP4 and HP5, respectively. Brazilian cement CP-V ARI with high early strength (equivalent to ASTM Type III) was used in this Stage. The fine aggregate was natural river sand passing through a 2.4-mm sieve. The coarse aggregate was crushed gneiss with maximum size (d_a) equal to 9.5 mm. A melamine sulphonate-type superplasticizer (Sikament 300) was used.

Along with the beam specimens, six 100×200 mm cylinders were cast for each Series. The average 28-day values of the compressive stress were 65 MPa (±7.3%) for Series B1 (mix HP3), 85 MPa (±8.3%) for Series B2 (mix HP4), 88 MPa (±2.5%) for Series B3 (mix HP5), 84 MPa (±6.3%) for Series B4 (mix HP4) and 82 MPa (±3.5%) for Series B5 (mix HP4). The concrete mixes HP3, HP4 and HP5 were designed to

Table 2
Values of G_F measured from specimens tested in Series A1 and A2

Series (concrete)	f'_c (MPa)	G_F (N/m)						Average G_F (N/m)	Coefficient of variation (%)
		Beam 1	Beam 2	Beam 3	Beam 4	Beam 5	Beam 6		
A1 (HP1)	48	125	110	147*	112	120	135*	116	8.8
A2 (HP2)	49	119	115	118	128	113	126	120	5.0

* Values not considered for computing average G_F.

exceed a 28-day compressive strength of 70, 90 and 110 MPa, respectively. The lower values achieved for the compressive strength in relation to the target compressive strength can be attributed to the type of aggregate (gneiss) used in the concrete mixes and its maximum size (9.5 mm). Differently from the normal-concrete, the compressive strength of high-strength concrete can be limited by the aggregate strength, as pointed by Darwin et al. [8], and by the size of the coarse aggregate, as shown in the work of Rao and Prasad [9].

The equipment used to test the beam specimens was the same as in Stage 1, with two channels for data acquisition and a load cell of 25 kN capacity. All the tests were controlled by the vertical displacement of the load cell. The loads were applied across the beam width through one hinge and two rollers. The rollers were placed over rigid bearing plates glued with epoxy in the concrete, with the minimum possible rolling friction. For all the beams, the notch was precast with an acrylic plate with the thickness of 2 mm. For the first three Series of tests, the notch depth a_0 was equal to 1/6 of the height of the beams. For these Series, a discontinuous transfer from the peak load to low values of the load had occurred and the softening branch of the load–deflection curve could not be completely recorded. A strategy to obtain complete load–deflection curves was to increase the depth of the notches to 1/3 of the height of the beams for Series B4 and B5. Satisfactory results were obtained using a deeper notch. Nevertheless, the results for the beams with height equal to 304.8 mm with deeper notches still happened to be unstable under direct displacement control.

Table 3 shows the values obtained for the fracture energy G_F according to the work-of-fracture method. G_F was measured only for Series B4 and B5, for specimens with height equal to 38.1, 76.2 and 152.4 mm, because only for these specimens that it was possible to record the complete load–deflection curve. The same considerations made in Stage 1, regarding the computation of the total energy W and the correction of the load–deflection curves at low loads were made for these tests.

Table 4 shows the corrected maximum loads for all the tested beams. The corrected maximum loads were obtained by adding half the beam self-weight to the measured peak load, in order to take the effect of the weight of the specimen into account for fracture energy determination (as in RILEM TC89-FMT [2]). The values denoted with an asterisk were inconsistent with the trend of the other tests and were not considered for the determination of the fracture energy. Therefore, it was not possible to compute the fracture energy for Series B3 because the peak load of the specimens with two different sizes (152.4 and 304.8 mm) were lower than expected. For Series B4 and B5, some beams were not tested due to the evidence of small flaws around the beam notch noticed during inspection before testing. These flaws can be attributed to problems during the compaction and handling of the specimens.

Table 3
Values of average G_F measured from specimens tested in Stages 2 (Series B) and 3 (Series C)

Series (concrete)	f'_c (MPa)	a_0/d	Average G_F (N/m)			
			Depth d (mm)			
			38.1	76.2	154.4	304.8
B4 (HP4)	84	0.333	132	170	183	NM
B5 (HP4)	82	0.333	112	168	208	NM
C2 (HP4)	78	0.167	108	123	135	145
C3 (HP5)	69	0.167	121	127	146	168
C4 (HP3)	78	0.167	NT	127	144	150
C5 (HP4)	88	0.167	140	153	185	219

NT = specimens not tested; NM = values not measured.

Table 4
Corrected maximum loads for Series B1 to B5 (Stage 2)

Series (concrete)	f'_c (MPa)	a_0/d	Depth d (mm)	Corrected maximum load P^0 (N)		
				Beam 1	Beam 2	Beam 3
B1 (HP3)	65	0.167	38.1	2073	2279	2299
			76.2	4096	4155	4539
			152.4	6471	6198	6711
			304.8	10495	10418	9602
B2 (HP4)	85	0.167	38.1	2193	2423	2709
			76.2	4053	4529	4563
			152.4	7734*	6329	7585*
			304.8	11042*	9551	9496
B3 (HP5)	88	0.167	38.1	2532	2663	2348
			76.2	4071	4692	4651
			152.4	5064*	3801*	5950*
			304.8	6249*	6611*	6522*
B4 (HP4)	84	0.333	38.1	1482	NT	NT
			76.2	2214	2101	NT
			152.4	3544	3266*	3794
			304.8	6480	6755	5589*
B5 (HP4)	82	0.333	38.1	1491	NT	NT
			76.2	2772	NT	NT
			152.4	3976	3694	3751
			304.8	7282*	6270	7299*

NT = specimens not tested.
* Values inconsistent with the trend of other tests.

The fracture energy obtained by the SEM was computed as specified in RILEM TC89-FMT [2]. Values of $g_f(\alpha_0)$ were computed equal to 6.07 and 14.20 for relative notch length equal to 0.167 and 0.333, respectively. The Young's modulus of elasticity was computed from the formula of Carrasquillo et al. [10] $E = 3320 f_c^{1/2} + 6900$ (MPa). The fracture parameters obtained from the regression analysis are shown in Table 5. As can be seem, only Series B1 and B2 comply the standard requirements concerning the limiting values of the coefficient of variation of the slope of the regression line (ω_A), the coefficient of variation of the intercept of the regression line (ω_C), and the relative width of scatter-band (m). The value of ω_A should not exceed 0.10 and the values of ω_C and m about 0.20. The values of ω_C for Series B5 and of ω_A for Series B4 are much higher than recommended. Nevertheless, the values found for G_f cannot be considered inconsistent when compared with the results of the other tests.

3.3. Results of stage 3

As in Stage 2, in Stage 3 [11] the dimensions of the beam specimens have scaled dimensions in order to permit the calculation of the fracture energy through the SEM besides the

Table 5
Fracture parameters obtained from the size effect method

Series	f'_c (MPa)	E (GPa)	a_0/d	$g_f(\alpha_0)$	A (mm^{-1} MPa^{-2})	G_f (N/m)	B (MPa)	d_0 (mm)	ω_A	ω_C	m
B1	65	33.7	0.167	6.07	0.00343	52.44	1.948	77	0.068	0.160	0.148
B2	85	37.5	0.167	6.07	0.00433	37.32	2.501	37	0.049	0.218	0.107
B4	84	37.3	0.333	14.20	0.00659	57.70	0.908	184	0.196	0.204	0.222
B5	82	37.0	0.333	14.20	0.00979	39.23	1.242	66	0.138	0.361	0.213
C2	78	36.2	0.167	6.07	0.00220	76.13	1.506	200	0.100	0.081	0.116
C3	69	34.5	0.167	6.07	0.00285	61.71	1.795	109	0.076	0.119	0.118
C4	78	36.2	0.167	6.07	0.00212	78.81	1.227	312	0.109	0.068	0.092
C5	88	38.0	0.167	6.07	0.00293	54.41	1.596	134	0.086	0.116	0.191

work-of-fracture method. The difference in relation to Stage 2 concerns to the type of equipment and displacement control used in the tests. A closed-loop servo-controlled Instron testing machine model 8502 with a load cell sensitive up to 50 kN was used this time. This machine has four channels for simultaneous data acquisition. All the specimens were tested under crack-mouth opening displacement (CMOD) control, which allowed the acquisition of load–CMOD and complete load–deflection curves for all specimen sizes.

The specimens had depths (d) of 38.1, 76.2, 152.4 and 304.8 mm, with the same thickness (b) of 38.1 mm, lengths equal to 2.67d, and span equal to 2.5d. A total of 72 beams, divided in five series of concrete batches (C1 to C5), were cast. For Series C1 to C4, three specimens were molded for

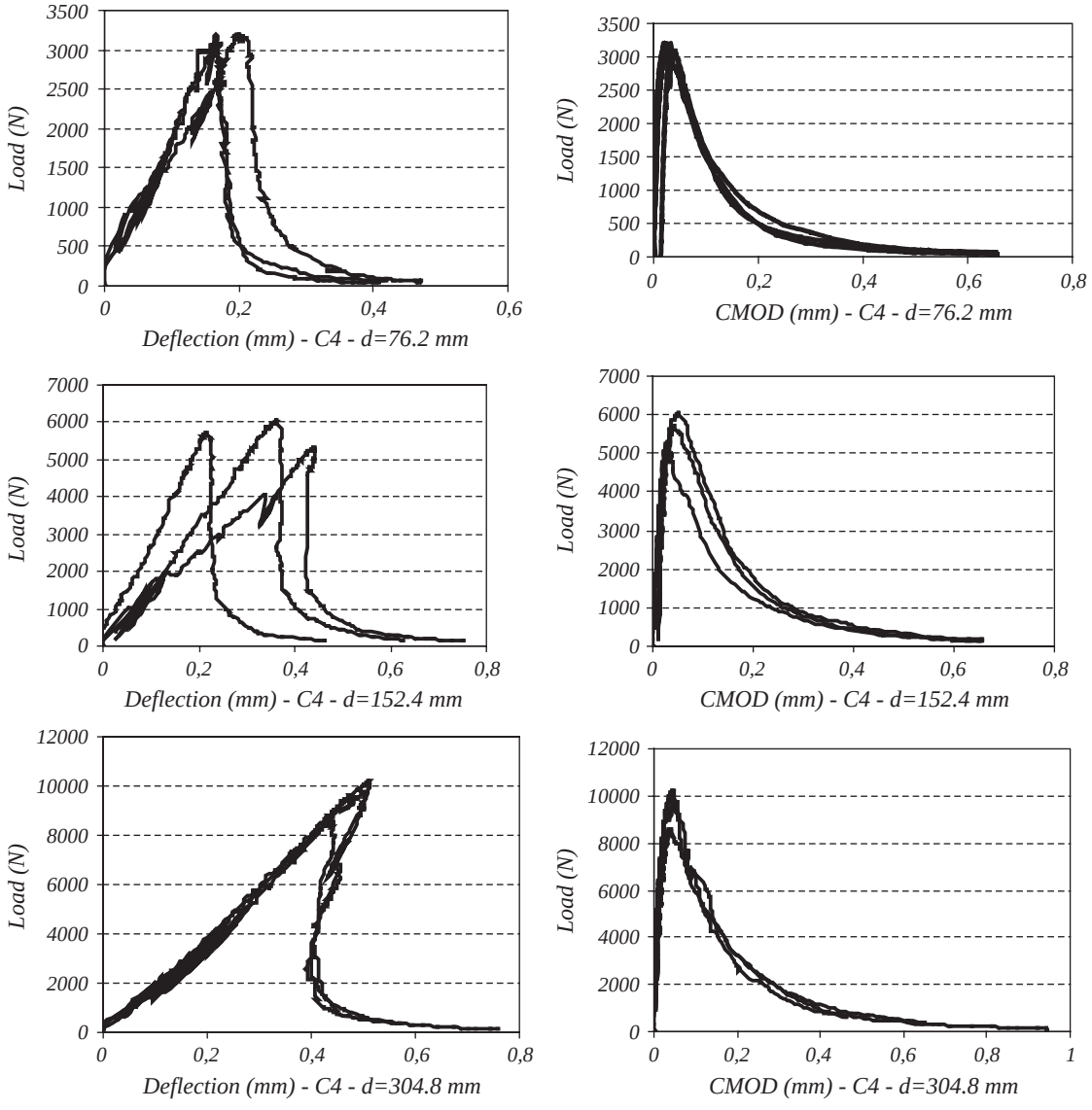

Fig. 2. Load–displacement (left) and load–CMOD (right) curves obtained for Series C4.

each of the four heights. For Series C5, six specimens were molded for each beam height. Series C1 was used to adjust the data acquisition equipment, the clip-gage and the velocity of the tests. Therefore, this Series will not be considered in the sequence of this paper. The concrete mixes HP3, HP4 and HP5 detailed in Table 1 were used in this Stage. The mix components have the same characteristics as described in Stage 2. Along with the beam specimens, six 100 × 200 mm cylinders were cast for each Series. The average 28-day values of the conventional compressive stress were 78 MPa (±3.1%) for Series C2 (mix HP4), 69 MPa (±2.2%) for Series C3 (mix HP5), 78 MPa (±3.5%) for Series C4 (mix HP3) and 88 MPa (±2.0%) for Series C5 (mix HP4). As in Stage 2, the lower values obtained in the cylinder tests in relation to the expected design strength can be attributed to the type and maximum diameter of the coarse aggregate used in the concrete mixes.

The beam specimens have the same notch depth for all Series, equal to 1/6 of the beam height. For Series C2, C3 and C4, the notches were precast with an acrylic plate with the thickness of 2 mm. For Series C5 the notches were saw-cut after curing. Load–deflection and load–CMOD diagrams for the specimens of Series C4 are presented in Fig. 2. One can verify the occurrence of snap-back behavior for larger samples.

The fracture energy G_F, measured according to the work-of-fracture method, is presented in Table 3. Table 6 shows the corrected maximum loads obtained for all the tested beams. The values denoted with an asterisk were inconsistent with the trend of the other tests and were not considered for the determination of the fracture parameters by the SEM. Some specimens were not tested due to flaws in the concrete, as in Stage 2.

The fracture energy obtained through the SEM was computed as in RILEM TC89-FMT [2] guidelines. Values of the non-dimensional energy release rate and the Young's modulus of elasticity were computed as in Stage 2. The fracture parameters obtained from the regression analysis are given in Table 5. As can be seen, all the Series tested at this Stage comply the standard requirements concerning to the limiting values of ω_A, ω_C, and m.

Table 6
Corrected maximum loads for Series C2 to C5 (Stage 3)

Series (concrete)	f'_c (MPa)	a_0/d	Depth d (mm)	Corrected maximum load P^0 (N)		
				Beam 1/4	Beam 2/5	Beam 3/6
C2 (HP4)	78	0.167	38.1	2086	1993	2043
			76.2	3517	3815	3719
			152.4	6802	6269	7680*
			304.8	12403*	11607	10591
C3 (HP5)	69	0.167	38.1	2151	2283	2393
			76.2	3710	3794	NT
			152.4	6963	7294	7912*
			304.8	10644	10522	NT
C4 (HP3)	78	0.167	38.1	NT	NT	NT
			76.2	3209	3200	3100
			152.4	5350*	5762	6128
			304.8	8726*	9906	10305
C5 (HP4)	88	0.167	38.1	2042	1952	2010
				1756	NT	NT
			76.2	3540	3996	4103
				4321	3695	NT
			152.4	6970	6702	5981
				6260	5845	NT
			304.8	9655	10656	9833
				10803	10282	NT

NT = specimens not tested.
* Values inconsistent with the trend of other tests.

4. Analysis of the results

From the results obtained in Stages 2 and 3 by the work-of-fracture method (see Table 2), it is possible to verify that the values obtained for the total fracture energy are greatly affected by the size of the specimen. Although this size effect could be strongly reduced enhancing the experimental procedures, as pointed by Guinea and co-workers [12,13], the application of the SEM in place of the work-of-fracture method has the main advantage of being not affected by this size dependence. If the fracture energy is to be considered a material property, as intended by many researchers, its value must be independent of size effect, which justifies the use of the so-called size effect method.

As pointed by Bazant [14,15], the fracture energies G_F, obtained by the work-of-fracture method and G_f obtained by the SEM are two different material characteristics. The total fracture energy G_F represents the area under the complete load–deflection curve, and the initial fracture energy G_f represents the area under the initial tangent of the softening curve. The SEM has the advantage of providing fracture parameters that are size and shape independent, with a lower scatter of results in comparison with the work-of-fracture method. On the other hand, the complete load–deflection curve is required most of the times in structural analysis, applied to concrete constitutive models when performing finite element analysis. Therefore, for practical purposes, it would be of interest to establish a relationship between the fracture energy obtained by the two processes. Bazant and Becq-Giraudon [16,17] verified statistically the approximated ratio $G_F/G_f \approx 2.5$, with a coefficient of variation around 40%, which allows the calibration of the complete softening curve from the results obtained by the SEM. From the data of Series B4, B5, C2, and C5 of the present study (same concrete mix), it was obtained the ratio $G_F/G_f = 2.88$, with a coefficient of variation equal to 38.1%. These values comply with the referred statistical study, given the uncertainty of the aforementioned ratio.

Some researches verified the relationship between fracture energy and compressive strength. Xie et al. [18] tested beam specimens by the work-of-fracture method and obtained average values for G_F that increases 13% and 11% for an increase of 53% and 29% in the compressive strength, respectively. Gettu et al. [19] compared results obtained for high-strength concrete and conventional concrete and verified that an increase of 160% in the compressive strength resulted in an increase of only 12% in the fracture energy. These numbers show the necessity of a relative great increase in the compressive strength in order to evidence a small increase in

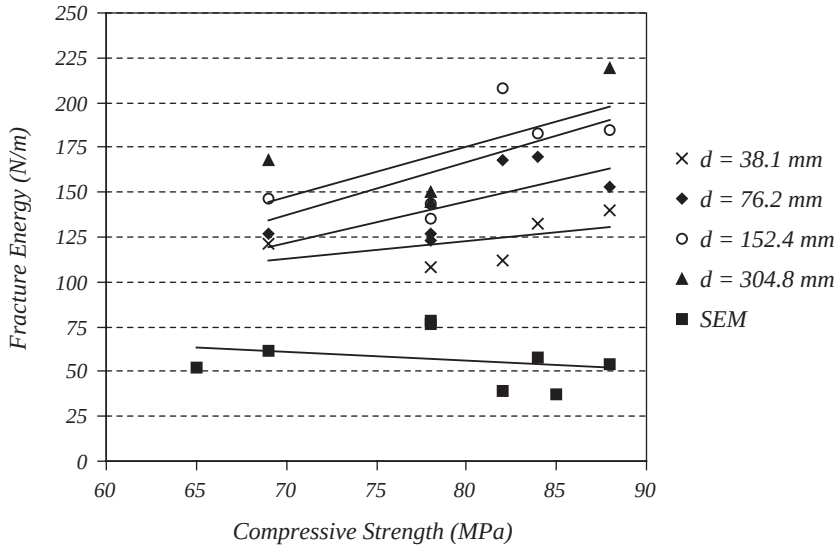

Fig. 3. Fracture energy versus compressive strength. The straight lines (from bottom to top) are related to SEM, d=38.1, 76.2, 152.4 and 304.8 mm, respectively.

the fracture energy. Some authors, as Rao and Prasad [9] and Gettu et al. [19], concluded that the fracture energy increases as the compressive strength of the concrete increases. Apparently, the results obtained in the present study follow this trend. Fig. 3 shows the least squares fit over the results obtained for G_F considering the data from Stages 2 and 3 grouped for specimens of the same size. For all the four sizes, an increase on fracture energy can be observed for increasing compressive strength. Nevertheless, the results obtained for G_f, also shown in Fig. 3, show a slight tendency to decrease with increasing compressive strength. This compares favorable with the results of Darwin et al. [8], who concluded that the concrete fracture energy is governed principally by the properties of the coarse aggregate and the fracture energy shows no clear relationship with the compressive strength.

Results obtained in Stage 1 (see Table 2) can be compared with some results obtained from literature for specimens with the same size and notch depth. The results seem to follow the same trend of higher fracture energy for higher values of the compressive strength. The mean value of 120 N/m for the fracture energy corresponding to a mean compressive strength of 48.5 MPa (Series A1 and A2) follows the sequence of results obtained by Xie et al. [18] with mean compressive strengths of 60, 92 and 119 MPa delivering fracture energy average values of 152, 172 and 191 N/m, respectively. The test results are also compatible with the results obtained by Rao and Prasad [9], who tested $100\times100\times500$ mm beam specimens with compressive strengths of 55, 63, 75 and 74 MPa and obtained fracture energy values of 122, 137, 151 and 165 N/m, respectively. Nevertheless, the value obtained by Ulfkjaer and Brincker [20] is contrary to this trend. They tested three HPC specimens with a mean compressive strength of 163 MPa to obtain the fracture energy average value of only 125 N/m.

Fig. 4 shows the size–effect plot of Series B2 and C4, which corresponds to the two extreme cases of brittle behavior found in the analysis. It can be seen that the test data lie close to the predictions of the size effect law. The brittleness numbers β were calculated according to Eq. (4) using the parameter d_0 presented in Table 5. The direct tensile strength was computed from the ACI [21] relation $f'_t = 0.59 f'^{1/2}_c$ (MPa). The results for normal strength concrete (NSC), picked up from the paper of Gettu et al. [22], for beams with heights (d) equal to 80, 160 and 320 mm and d_0=363 (compare with heights 76, 152 and 305 of the present study), are also plotted for comparison. It can be seen that Series B2 presents a higher brittle behavior than the conventional concrete. Nevertheless, the values for Series C4 are unexpected closer to the values obtained for the conventional concrete. Generally, a lower value of d_0 and a higher value of B indicate higher brittleness and higher strength, respectively. One can expect higher brittleness corresponding to higher compressive strength. Analyzing the values given in Table 5, it is not possible to verify this assumption. The results obtained for the parameter d_0 were very sparse and did not permit any conclusions. The parameter B showed a tendency to decrease as the concrete strength increases, which is contrary to the expected trend.

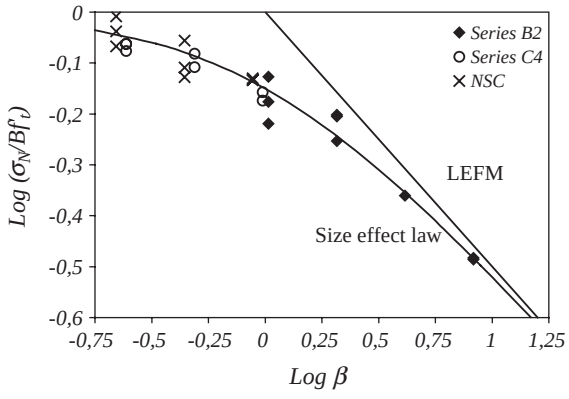

Fig. 4. Size effect plot of Series B2, C4 and conventional concrete (NSC).

5. Conclusions

Three-point bend notched beams were tested at the Technological Institute at PUC-Rio (ITUC) in order to study the fractures properties of HPC. The main conclusions that can be drawn from this study are the following:

1. The results obtained by the work-of-fracture method apparently follow the trend of fracture energy increasing as the compressive strength of the concrete increases. Nevertheless, the results for fracture energy obtained by the SEM shows a slight trend to decrease with increasing compressive strength.
2. The range of brittleness numbers found in this study shows that HPC structures must be designed using the nonlinear fracture mechanics, at least for normal size structures.
3. The results obtained for the parameter d_0 were very sparse and did not allow any conclusions regarding the brittleness behavior. The fracture parameter B showed a trend contrary to the expected, presenting a slight decrease in value as compressive strength increases.
4. The ratio G_F/G_f between the fracture energy measured by the work-of-fracture method and the SEM was found equal to 2.88 for the specimens cast with the same type of concrete, with a coefficient of variation equal to 38.1%. These values comply with the statistical study carried out by Bazant and Becq-Giraudon [16,17].
5. The results obtained from the standard compressive strength tests indicate that the concrete strength was limited by the type and size of the coarse aggregate (gneiss). This type of aggregate is usually applied in Brazil. Nevertheless, more specific experiments must be carried out in order to verify this assumption.

Acknowledgments

The authors wish to acknowledge the financial support of the Brazilian agency CNPq (National Council for Technological and Scientific Development) that made this work possible.

References

[1] RILEM 50-FMC, RILEM Draft Recomm. 18 (106) (1985) 285.
[2] RILEM TC89-FMT, Mat. Struct. 23 (1990) 461.
[3] Z.P. Bazant, P.A. Pfeiffer, ACI Mater. J. (1987 (November–December)) 463.
[4] A. Hillerborg, Mat. Struct. 18 (106) (1985) 291.
[5] T.L. Anderson, Fracture Mechanics — Fundamentals and Applications, CRC Press, Boca Raton, FL, USA, 1991.
[6] G. Rodrigues, Determination of the Fracture Energy for High-Performance Concrete, MSc Thesis (in Portuguese), Department of Civil Engineering, PUC-Rio, Rio de Janeiro, Brazil, (1998).
[7] M.L.O. Silva, Experimental Study on Fracture Energy and Size-Effect of High-Performance Concrete, MSc Thesis (in Portuguese), Department of Civil Engineering, PUC-Rio, Rio de Janeiro, Brazil, (2000).
[8] D. Darwin, S. Abraham, R. Kosul, S.G. Luan, ACI Mater. J. 98 (5) (2001) 410.
[9] G.A. Rao, B.K.R. Prasad, Cem. Concr. Res. 32 (2) (2002) 247.
[10] R.L. Carrasquillo, A.H. Nilson, F.O. Slate, ACI J. Proc. 78 (3) (1981) 171.
[11] V.S. Caland, Experimental Results of Fracture Parameters for High-Performance Concrete, MSc Thesis (in Portuguese), Department of Civil Engineering, PUC-Rio, Rio de Janeiro, Brazil, (2001).
[12] G.V. Guinea, J. Planas, M. Elices, Mat. Struct. 25 (1992) 212.
[13] J. Planas, M. Elices, G.V. Guinea, Mat. Struct. 25 (1992) 305.
[14] Z.P. Bazant, Q. Yu, Z. Zi, Int. J. Fract. 118 (2002) 303.
[15] Z.P. Bazant, J. Planas, Fracture and Size Effect in Concrete and Other Quasibrittle Materials, CRC Press, Boca Raton, 1998.
[16] Z.P. Bazant, E. Becq-Giraudon, in: R. de Borst, J. Mazars, G. Pijaudier-Cabot, J.G.M. van Mier (Eds.), Proc. FranMCoS-4 Int. Conf., Paris, A.A. Balkema Publishers, Lisse, 2001, p. 491.
[17] Z.P. Bazant, E. Becq-Giraudon, Cem. Concr. Res. 32 (4) (2002) 529.
[18] J. Xie, A.E. Elwi, J.G. MacGregor, ACI Mater. J. 92 (2) (1995) 135.
[19] R. Gettu, Z.P. Bazant, M.E. Karr, ACI Mater. J. 87 (6) (1990) 608.
[20] J.P. Ulfkjaer, R. Brincker, in: F.H. Wittmann (Ed.), Proceedings FRAMCOS-2, vol. 1, 1995, p. 31.
[21] ACI Committee 363, ACI Report 363R-92, American Concrete Institute, Farmington Hills, MI, 1992, p. 1.
[22] R. Gettu, H. Saldivar, M.T. Kazemi, Int. J. Solids Struct. 35 (31–32) (1998) 4121.